Chromium oxide supported on mesoporous SBA-15 as propane dehydrogenation and oxidative dehydrogenation catalysts

Xuezheng Zhang, Yinghong Yue, and Zi Gao *

Laboratory of Molecular Catalysis and Innovative Materials, Department of Chemistry,
Fudan University, Shanghai 200433, P.R. China

Received 14 March 2002; accepted 27 May 2002

The catalytic activity and selectivity of Cr_2O_3 supported on mesoporous SBA-15 for non-oxidative and oxidative dehydrogenation of propane by O_2 and CO_2 have been studied and compared with those of Cr_2O_3/ZrO_2 and $Cr_2O_3/\gamma\text{-}Al_2O_3$ catalysts. Cr_2O_3/SBA-15 and Cr_2O_3/ZrO_2/SBA-15 are more selective to propene and more resistant to coking in comparison with Cr_2O_3/ZrO_2 and $Cr_2O_3/\gamma\text{-}Al_2O_3$ for non-oxidative dehydrogenation of propane. In oxidative dehydrogenation of propane by O_2 and CO_2, Cr_2O_3/SBA-15 also displays better activity, selectivity and stability than the other two supported catalysts. The propane conversion and propene yield on Cr_2O_3/SBA-15 catalyst for oxidative dehydrogenation of propane by CO_2 at 823 K reach 24.2 and 20.3%, respectively. XPS and TG/DTA have been used to characterize the catalysts before and after reaction. The differences in catalytic behavior of various supported Cr_2O_3 catalysts in the reactions have been discussed on the basis of the characterization results.

KEY WORDS: SBA-15-supported Cr_2O_3 catalyst; C_3H_8 dehydrogenation; C_3H_8 oxidative dehydrogenation by O_2; C_3H_8 oxidative dehydrogenation by CO_2.

1. Introduction

Propane is an important raw material for the production of polypropylene, polyacrylonitrile, acrolein and acrylic acid. The catalytic dehydrogenation of propane is of commercial interest, because the production of propene from steam cracking and FCC is not sufficient to meet the increasing needs of the market. Chromia supported on various oxides, such as $\gamma\text{-}Al_2O_3$, SiO_2 and ZrO_2, are well-known active catalysts for this reaction [1–5].

Alkane dehydrogenation is a highly endothermic reaction, which requires high reaction temperature and is thermodynamically limited by equilibrium. Thermal cracking side reactions of hydrocarbons are favored at high temperatures, leading to a significant increase in the production of lighter alkanes and coke. As a consequence, the dehydrogenation catalysts are rather non-selective and unstable. Hence, the exothermic oxidative dehydrogenation of propane by oxygen as an alternative process has recently become the object of many investigations. The more active and selective catalysts reported in the literature for oxidative dehydrogenation of propane by oxygen are supported oxides of V, Ti, Mo, Mn and Cr [6–14]. However, selectivity of this reaction is rather low due to the over-oxidation of propane to carbon oxides. More recently, carbon dioxide as one of the major greenhouse gases has been utilized in several partial oxidation reactions, such as reforming and oxidative coupling of methane. The oxidative dehydrogenation of propane by carbon dioxide over supported chromium catalysts has also been reported as giving rather high propene selectivity [15,16].

SBA-15 is a newly-reported silica mesoporous material with high specific surface area and large pore size prepared by using a triblock copolymer as a template [17]. It has a more regular structure and a thicker channel wall than MCM-41, resulting in much higher thermal stability. These unique properties of SBA-15 have made the material desirable for application as catalyst supports. In this work, the results of the study on the catalytic behavior of SBA-15-supported chromia catalysts for dehydrogenation and oxidative dehydrogenation of propane by oxygen and carbon dioxide are reported and compared with other supported chromia catalysts.

2. Experimental

2.1. Catalysts

SBA-15 mesoporous material was prepared following the procedures in the literature [18]. 2 g of triblock poly(ethylene oxide)-poly(propylene oxide)-poly(ethylene oxide) ($EO_{20}PO_{70}EO_{70}$, Aldrich) was added into 80 ml of 2 mol l^{-1} HCl solution and stirred at 313 K for 3 h. Then, 4.25 g tetraethyl orthosilicate (TEOS) was added and stirred for 2 h. The mixture was allowed

---

* To whom correspondence should be addressed.
E-mail: zigao@fudan.edu.cn

to react at 373 K for 48 h. The precipitate was filtered, dried and calcined in air flow at 773 K for 5 h.

The supported oxide catalysts were prepared by impregnating the relevant amount of chromium nitrate and/or zirconium nitrate solution on SBA-15 or other supports using an incipient wetness method. The impregnated samples were dried at 383 K and calcined at 823 K in air flow for 5 h. The catalysts were designated as metal oxide(x)/support, where x represented the weight percentage of the metal oxide in the catalysts.

2.2. Characterization

X-ray powder diffraction (XRD) patterns were obtained on a Rigaku D/MAX-IIA diffractometer using Cu K_α radiation at 30 kV and 20 mA. BET surface area and pore volume were measured under liquid nitrogen temperature on a Micromeritics ASAP-2000 instrument using N_2 as the adsorbent. Thermal analysis (TG/DTA) was carried out on a Rigaku Thermoflex instrument. 10–20 mg of sample was heated from room temperature to 873 K at a heating rate of 10 K min^{-1} in flowing air. X-ray photoelectron spectra (XPS) were obtained with a Perkin-Elmer PHI-5000 ESCA system using Mg K_α radiation at 14 kV and 250 W. The vacuum of the specimen chamber was better than 5×10^{-7} Pa, and C 1s at 284.6 eV was taken as reference.

2.3. Catalytic test

Catalytic tests were performed in a fixed-bed flow microreactor at ambient pressure, and the catalyst load was 200 mg. Nitrogen was used as the carrier gas at a flow rate of 20 ml min^{-1}. For non-oxidative dehydrogenation of propane, the catalysts were pretreated at 823 K for 0.5 h in oxygen flow, and then at 623 K for 0.5 h in hydrogen flow. The gas reaction mixture contained 2.5 mol% propane and balancing nitrogen, and the reaction temperature was 823 K. For oxidative dehydrogenation of propane by oxygen, the catalysts were pretreated at 823 K for 1 h in nitrogen flow. The reaction mixture contained 2.5 mol% propane, 2.5 mol% oxygen and balancing nitrogen, and the reaction temperature was 723 K. For oxidative dehydrogenation of propane by carbon dioxide, the catalysts were pretreated at 823 K for 0.5 h in oxygen flow, and then at 623 K for 0.5 h in hydrogen flow. The reaction mixture contained 2.5 mol% propane, 2.5 or 5.0 mol% carbon dioxide and balancing nitrogen, and the reaction temperature was 823 K.

The hydrocarbon reaction products were analyzed using an on-line gas chromatograph equipped with a 6 m column of Porapak Q and a flame ionization detector (FID). The gas products, such as N_2, O_2, CO, CH_4 and CO_2, were analyzed using another on-line gas chromatograph equipped with a 2 m packed column of carbon molecular sieve 601 and a thermal conductance detector (TCD).

3. Results and discussion

3.1. Propane dehydrogenation on different supported Cr_2O_3 catalysts

A series of Cr_2O_3/ZrO_2 catalysts with different Cr_2O_3 loading were prepared and tested. The main reaction products of propane dehydrogenation are C_3H_6 and H_2, and the minor reaction products are CH_4, C_2H_4 and CO. The activity and selectivity of the catalysts at 10 min and 360 min are listed in table 1 along with the values of BET surface area and pore volume of the catalysts. All the Cr_2O_3/ZrO_2 catalysts undergo a fast deactivation process, but the propene selectivity of the catalysts increases with reaction time. On the other hand, the propane conversion and propene yield increase as Cr_2O_3 loading increases and they reach a plateau

Table 1
Results of propane dehydrogenation on supported Cr_2O_3 catalysts at 823 K.

Catalyst	Conversion (%)		C_3H_6 selectivity (%)		C_3H_6 yield (%)		S_{BET} ($m^2\,g^{-1}$)	V ($cm^3\,g^{-1}$)
	10 min	360 min	10 min	360 min	10 min	360 min		
Cr_2O_3(0.6)/ZrO_2	40.4	24.0	81.2	90.4	32.8	21.7	57	0.27
Cr_2O_3(2)/ZrO_2	59.3	25.7	77.8	88.7	46.1	22.8	47	0.18
Cr_2O_3(4)/ZrO_2	60.9	24.3	76.2	87.0	46.4	21.1	43	0.17
Cr_2O_3(8)/ZrO_2	58.5	25.9	77.6	82.5	45.4	21.4	42	0.16
Cr_2O_3(2)/Al_2O_3	12.1	8.81	92.4	93.8	11.2	8.27	100	0.41
Cr_2O_3(2)/SBA-15	30.4	18.1	90.7	96.0	27.6	17.4	591	0.61
Cr_2O_3(0.6)/ZrO_2(30)/SBA-15	13.8	7.60	97.8	98.2	13.5	7.46	292	0.35
Cr_2O_3(1.2)/ZrO_2(30)/SBA-15	25.8	15.1	95.3	96.1	24.6	14.5	251	0.32
Cr_2O_3(2)/ZrO_2(30)/SBA-15	32.9	20.9	93.7	93.1	30.8	19.4	238	0.29
Cr_2O_3(4)/ZrO_2(30)/SBA-15	32.8	20.2	86.0	89.8	28.2	18.2	216	0.24

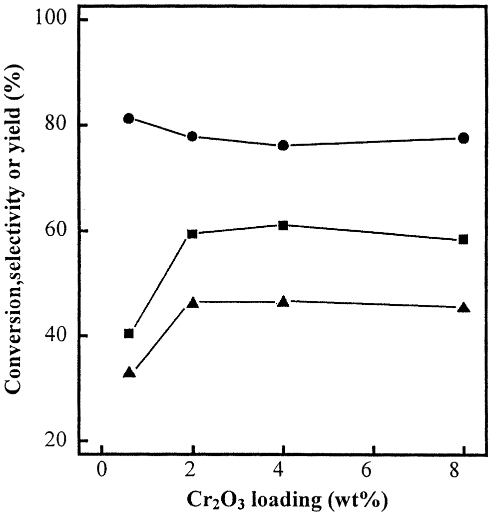

Figure 1. Dependence of initial activity and selectivity on Cr_2O_3 loading for Cr_2O_3/ZrO_2 catalysts. (■) C_3H_8 conversion; (●) C_3H_6 selectivity; (▲) C_3H_6 yield.

above 2 wt% Cr_2O_3, whereas the propene selectivity is not so sensitive to the Cr_2O_3 content of the catalysts. The dependence of initial activity and selectivity of Cr_2O_3/ZrO_2 catalysts on Cr_2O_3 loading is shown in figure 1.

The effect of support on the catalytic behavior of chromia catalysts in dehydrogenation of propane was also investigated. The reaction data of $Cr_2O_3(2)/ZrO_2$, $Cr_2O_3(2)/\gamma$-Al_2O_3 and $Cr_2O_3(2)$/SBA-15 are listed in table 1, and the variation of propene yield with time on stream for the catalysts is illustrated in figure 2. The propene yield of the supported catalysts with the same Cr_2O_3 loading follows the order of $Cr_2O_3(2)/ZrO_2 >$ $Cr_2O_3(2)$/SBA-15 $> Cr_2O_3(2)/\gamma$-Al_2O_3. Moreover, these catalysts exhibit different deactivation rates. The most active Cr_2O_3/ZrO_2 deactivates faster than the other two catalysts.

TG/DTA profiles of $Cr_2O_3(2)/ZrO_2$ and $Cr_2O_3(2)$/SBA-15 catalysts after reacting for 6 h are illustrated in figure 3. The exothermic peak at 583–589 K for the catalysts corresponds to burning of coke deposit, and the endothermic peak at 345 K for $Cr_2O_3(2)$/SBA-15 corresponds to desorption of adsorbed water [19]. The amount of carbon deposit on the used $Cr_2O_3(2)/ZrO_2$ and $Cr_2O_3(2)$/SBA-15 catalysts measured by TG is 1.6 and 0.7 wt%, respectively. The higher coking rate of $Cr_2O_3(2)/ZrO_2$ may account for its faster deactivation in the reaction.

XRD patterns of the fresh and used $Cr_2O_3(2)$/SBA-15 catalysts in the low-angle region are given in figure 4, showing that the mesostructure of SBA-15 remains intact after 6 h reaction at 823 K.

The XPS spectra of C 1s for the same used $Cr_2O_3(2)/ZrO_2$ and $Cr_2O_3(2)$/SBA-15 catalysts are illustrated in figure 5. The amount of carbon deposit on the surface of $Cr_2O_3(2)/ZrO_2$ is obviously greater than that on

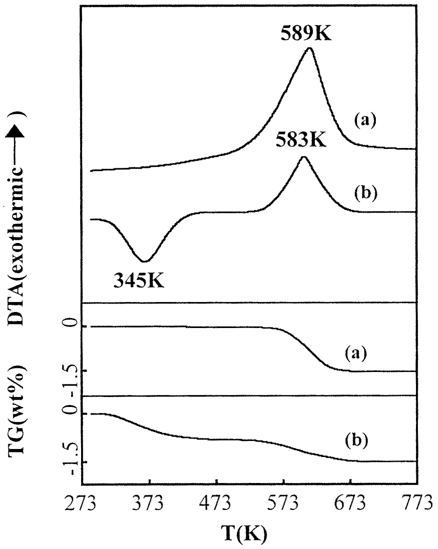

Figure 3. TG-DTA profiles of used catalysts. (a) $Cr_2O_3(2)/ZrO_2$; (b) $Cr_2O_3(2)$/SBA-15.

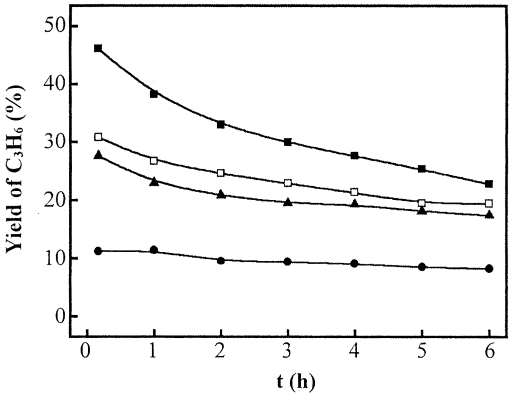

Figure 2. Propane yield of supported Cr_2O_3 catalysts as a function of time on stream. (■) $Cr_2O_3(2)/ZrO_2$; (▲) $Cr_2O_3(2)$/SBA-15; (●) $Cr_2O_3(2)/\gamma$-Al_2O_3; (□) $Cr_2O_3(2)/ZrO_2(30)$/SBA-15.

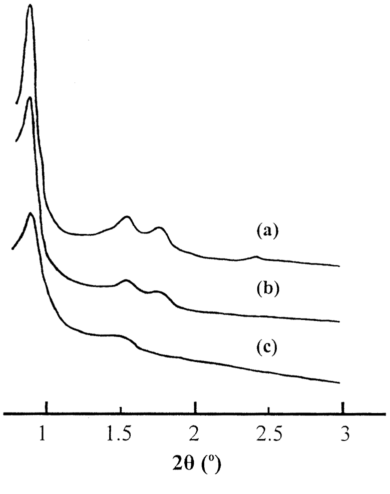

Figure 4. XRD patterns of samples. (a) SBA-15; (b) $Cr_2O_3(2)$/SBA-15 (fresh); (c) $Cr_2O_3(2)$/SBA-15 (used).

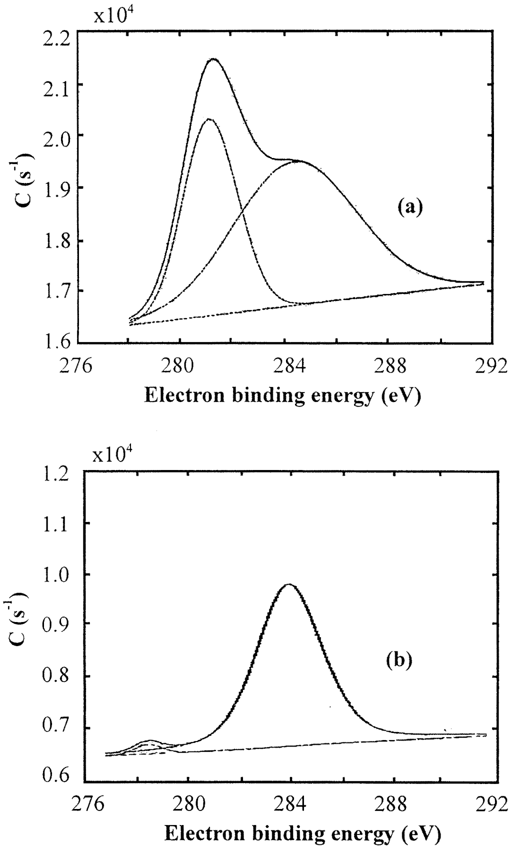

Figure 5. XPS spectra of C 1s for catalysts after 6 h reaction. (a) Cr_2O_3(2)/ZrO_2; (b) Cr_2O_3(2)/SBA-15.

Cr_2O_3(2)/SBA-15. Furthermore, a new peak appears at 281.1 and 278.5 eV on the spectra of Cr_2O_3(2)/ZrO_2 and Cr_2O_3(2)/SBA-15, respectively, besides the characteristic peak of C 1s at 284.6 eV, indicating that carbidic carbon is present on the surface of the catalysts. The high intensity of this peak on the XPS spectrum of Cr_2O_3(2)/ZrO_2 shows that the formation of chromium carbide is favored. The greater loss of surface chromium active sites due to the formation of carbide on the catalyst again explains the faster deactivation of Cr_2O_3(2)/ZrO_2 catalyst in non-oxidative dehydrogenation of propane.

3.2. *Propane dehydrogenation on Cr_2O_3/ZrO_2/SBA-15 catalysts*

The above experimental results show that chromia on ZrO_2 and SBA-15 displays higher propene yield in propane dehydrogenation in comparison with the widely employed chromia on γ-Al_2O_3. The presence of weak acidic and basic sites on ZrO_2 [3] and the high surface area of SBA-15 may have positive effects on the catalytic performance of the catalysts. Hence, chromia supported on ZrO_2-coated SBA-15 catalysts were prepared and investigated in this work to see if a synergism of these unique features of the two supports could appear.

XRD patterns of SBA-15 coated with different amounts of ZrO_2 after calcination at 823 K are illustrated in figure 6. In the low-angle region, SBA-15 exhibits one intense line and two weak lines, which can be indexed to the (100), (110) and (200) diffraction lines characteristic of its hexagonal structure [18]. The XRD patterns of the ZrO_2 coated SBA-15 samples give the same diffraction lines in the low-angle region, indicating that the structure of the mesoporous silica is intact after coating. No clear diffraction lines are observed in the wide-angle region for samples with ZrO_2 loading below 30 wt%, implying that ZrO_2 is highly dispersed on the surface of SBA-15. For samples with ZrO_2 loading above 30 wt%, low and broad lines that can be indexed to (111), (202) and (131) diffraction lines of tetragonal ZrO_2 appear on the patterns, showing that small zirconia crystallites start to form on the surface of SBA-15. Hence, ZrO_2(30)/SBA-15 was selected as an appropriate support in the present work.

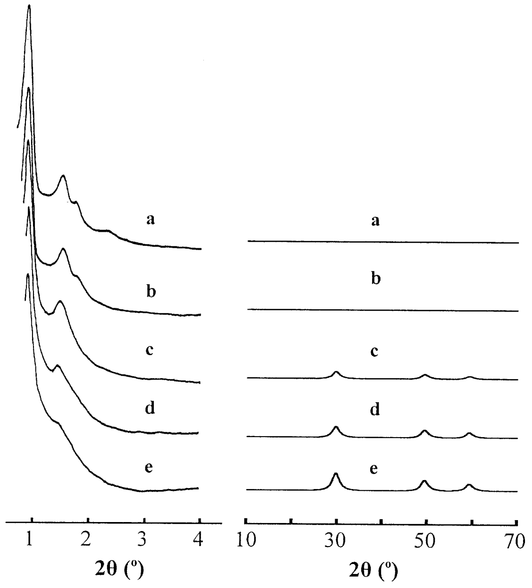

Figure 6. XRD patterns of ZrO_2 coated SBA-15 samples calcined at 823 K. (a) SBA-15; (b) ZrO_2(20)/SBA-15; (c) ZrO_2(30)/SBA-15; (d) ZrO_2(40)/SBA-15; (e) ZrO_2(50)/SBA-15.

The activity and selectivity of Cr_2O_3/ZrO_2(30)/SBA-15 catalysts with different Cr_2O_3 loading for propane dehydrogenation at 10 and 360 min are listed in table 1. The dependence of initial activity and selectivity on Cr_2O_3 loading for this series of catalysts is similar to that for Cr_2O_3/ZrO_2 catalysts, as shown in figure 7. The propane conversion and propene yield of the catalysts reach a plateau as the Cr_2O_3 loading is above 2 wt%. The variation of propane conversion, propene selectivity and yield with time on stream on Cr_2O_3(2)/ZrO_2(30)/SBA-15 catalyst is illustrated in figure 2 and compared with the other supported chromia catalysts with the same amount of Cr_2O_3 loading. The catalytic performance of Cr_2O_3(2)/ZrO_2(30)/SBA-15 is obviously somewhat in-between Cr_2O_3(2)/ZrO_2 and Cr_2O_3(2)/SBA-15. It is less active, but more selective and stable than Cr_2O_3(2)/ZrO_2 catalyst. After 6 h reaction, the

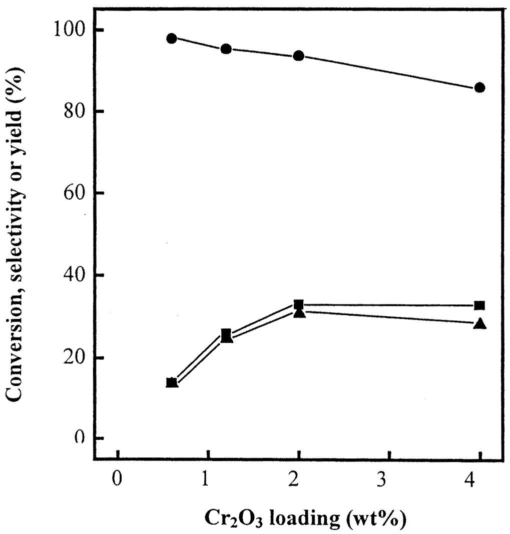

Figure 7. Dependence of initial activity and selectivity on Cr_2O_3 loading for $Cr_2O_3/ZrO_2(30)$/SBA-15 catalysts. (■) C_3H_8 conversion; (●) C_3H_6 selectivity; (▲) C_3H_6 yield.

propene yield of $Cr_2O_3(2)/ZrO_2$, $Cr_2O_3(2)/ZrO_2(30)$/SBA-15 and $Cr_2O_3(2)$/SBA-15 is 22.8, 19.4 and 17.4%, respectively.

The TG/DTA profile of $Cr_2O_3(2)/ZrO_2(30)$/SBA-15 catalyst after 6 h reaction is similar to that of $Cr_2O_3(2)$/SBA-15. The exothermic peak for burning of carbon deposit appears at 587 K, and the amount of carbon deposit on $Cr_2O_3(2)/ZrO_2(30)$/SBA-15 is 0.8 wt%.

3.3. *Oxidative dehydrogenation of propane by O_2 on supported Cr_2O_3 catalysts*

The steady-state activity and selectivity of different supported Cr_2O_3 catalysts for oxidative dehydrogenation of propane by O_2 at 723 K after 6 h on stream are given in table 2. The main reaction products are C_3H_6 and CO_x, and traces of CH_4 and C_2H_4 are also detected in a few cases. In general, the propene selectivity and yield in the reaction are rather low due to over-oxidation of the reactant to CO_x. However, $Cr_2O_3(2)$/SBA-15 is the most active catalyst for this reaction, and the propene yield of the catalysts decreases in the order of $Cr_2O_3(2)$/SBA-15 > $Cr_2O_3(2)/ZrO_2(30)$/SBA-15 > $Cr_2O_3(2)/\gamma\text{-}Al_2O_3$ > $Cr_2O_3(2)/ZrO_2$.

Pretreating $Cr_2O_3(2)$/SBA-15 catalyst at 823 K in O_2 flow and then at 623 K in H_2 flow improves its catalytic activity and selectivity in the oxidative dehydrogenation reaction. The highest propene yield observed on $Cr_2O_3(2)$/SBA-15 catalyst is 4.75%, which is slightly higher than those reported in literature for Cr_2O_3 supported on MCM-41 [13] and on zirconium- and lanthanum-doped MCM-41 [14]. However, the low propene yield on the catalysts is no doubt the main problem of concern for this catalytic reaction in competition with the non-oxidative dehydrogenation process.

3.4. *Oxidative dehydrogenation of propane by CO_2 on supported Cr_2O_3 catalysts*

Carbon dioxide is a milder oxidant. It has been reported that CO_2 enhances the yield of propene on Cr_2O_3/SiO_2 catalyst and suppresses catalyst deactivation [15]. Hence, oxidative dehydrogenation of propane by CO_2 on various supported Cr_2O_3 catalysts were studied. The steady-state reaction data at 823 K are given in table 3. In this reaction $Cr_2O_3(2)$/SBA-15 is more active than $Cr_2O_3(2)/SiO_2$ and $Cr_2O_3(2)/\gamma\text{-}Al_2O_3$ and less active than $Cr_2O_3(2)/ZrO_2$, but it is more selective to propene than all the other catalysts. The propene yield on $Cr_2O_3(2)$/SBA-15 in oxidative dehydrogenation by CO_2 at 823 K reaches 20.3%, which is almost equivalent to the propene yield on $Cr_2O_3(2)/ZrO_2$ catalysts in non-oxidative dehydrogenation at the same temperature (see table 1), but the catalyst is more stable in the presence of CO_2. The initial propene yield on $Cr_2O_3(2)$/SBA-15 is 22.5% and after 6 h on stream the steady-state propene yield is 20.3%. The amount of carbon deposit on $Cr_2O_3(2)$/SBA-15 after reacting for 6 h in the presence of CO_2 measured by TG-DTA is only 0.2%, which is much lower than that on $Cr_2O_3(2)/ZrO_2$ and $Cr_2O_3(2)$/SBA-15 in the absence of CO_2.

Coating SBA-15 with ZrO_2 reduces the activity and selectivity of the catalyst in oxidative dehydrogenation of propane by CO_2, but the propene selectivity on $Cr_2O_3(2)/ZrO_2(30)$/SBA-15 is still higher than that on

Table 2

Results of oxidative dehydrogenation of propane by O_2 on supported Cr_2O_3 catalysts at 723 K.

Catalyst	Conversion (%)	Selectivity (%)					C_3H_6 yield (%)
		C_3H_6	CO	CO_2	CH_4	C_2H_4	
$Cr_2O_3(2)/ZrO_2$	19.4	1.54	7.57	90.9	–	–	0.30
$Cr_2O_3(2)/\gamma\text{-}Al_2O_3$	22.2	8.06	25.4	66.6	–	–	1.78
$Cr_2O_3(2)$/SBA-15	24.2	12.5	25.5	60.0	0.85	1.15	3.03
$Cr_2O_3(2)/ZrO_2(30)$/SBA-15	26.6	7.22	14.2	78.5	–	–	1.92
$Cr_2O_3(2)$/SBA-15[a]	29.7	16.0	20.2	62.4	0.78	0.69	4.75

[a] The catalyst was pretreated at 823 K for 0.5 h in O_2 flow and then at 623 K for 0.5 h in H_2 flow.

Table 3
Results of oxidative dehydrogenation of propane by CO_2 on supported Cr_2O_3 catalysts at 823 K.

Catalyst	CO_2/C_3H_8 (molar ratio)	Conversion (%) C_3H_8	Selectivity (%)					C_3H_6 yield (%)
			C_3H_6	CH_4	C_2H_4	C_2H_6	CO	
$Cr_2O_3(2)/ZrO_2$	2	30.7	54.5	6.59	0.92	–	38.1	16.7
$Cr_2O_3(2)/\gamma\text{-}Al_2O_3$	2	9.67	79.4	3.35	–	–	17.2	7.68
$Cr_2O_3(2)/SiO_2$ [a]	2	19.1	76.7	1.93	2.83	–	18.5	14.7
$Cr_2O_3(2)$/SBA-15	2	24.2	83.9	1.82	3.33	–	10.9	20.3
$Cr_2O_3(2)/ZrO_2(30)$/SBA-15	2	22.7	63.3	1.35	0.68	–	34.7	14.4
$Cr_2O_3(2)$/SBA-15	1	12.6	87.6	1.64	2.36	–	8.44	11.0
$Cr_2O_3(4)$/SBA-15	1	20.7	86.0	1.67	2.36	2.23	7.76	17.8

[a] The specific surface area and pore volume of the catalyst are 263 $m^2\,g^{-1}$ and 0.59 $cm^3\,g^{-1}$, respectively.

$Cr_2O_3(2)/ZrO_2$. Moreover, the activity of $Cr_2O_3(2)$/SBA-15 decreases with decreasing CO_2/C_3H_8 molar ratio, as shown in table 3.

Cr_2O_3/SBA-15 catalysts display excellent activity, selectivity and stability in oxidative dehydrogenation of propane by CO_2. As a hopeful alternative to the process of non-oxidative dehydrogenation of propane, the oxidative dehydrogenation of propane by CO_2 on this type of catalyst deserves more systematic studies in the future.

3.5. XPS result

The XPS spectra in the Cr $2p_{3/2}$ region of the catalysts before and after 6 h on stream were recorded and deconvoluted into various components. The samples were pretreated in the same way as that before the catalyst test or kept in a hydrogen atmosphere after reaction. Figure 8 displays the XPS curves of $Cr_2O_3(2)$/SBA-15 before and after reaction as representative examples. The binding energy and percentage of the Cr species, Cr(II), Cr(III), Cr(V) and Cr(VI), on the catalysts are listed in table 4. The surface composition of the catalysts with the same Cr_2O_3 loading differs from one to another, implying that different interactions between chromia and the supports exist.

It has been suggested in the literature [4] that Cr(III) species are the active sites for dehydrogenation of propane and that Cr(II) species do not play any role in the reaction. Also, ESR study of ^{53}Cr-enriched sample [20] shows that Cr(III) species arising from reduction of Cr(V) are more active for dehydrogenation due to the formation of monomeric Cr(III) active sites. The unique high concentration of Cr(V) species on the surface of $Cr_2O_3(2)/ZrO_2$ resulting from a strong interaction between chromia and the basic support is probably responsible for its high activity in the dehydrogenation of propane.

On the other hand, XPS results demonstrate that the change in surface composition of the catalysts after 6 h on stream is dependent both on the nature of the support and the reaction conditions. For $Cr_2O_3(2)$/SBA-15 catalysts, in the absence of oxidant a considerable amount of Cr(III) species is reduced to inactive Cr(II) species by H_2 in the dehydrogenation reaction, whereas the concentration of Cr(III) species on the catalyst is almost unchanged in the presence of CO_2 and is increased in the presence of O_2. The effect of oxidant on surface composition during reaction may explain the slow deactivation of the catalyst in oxidative dehydrogenation of propane by O_2 or CO_2.

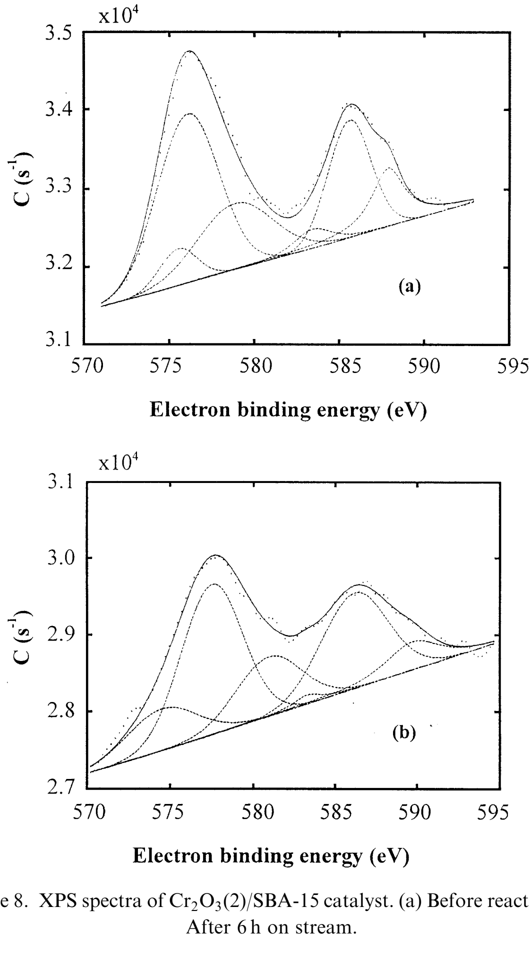

Figure 8. XPS spectra of $Cr_2O_3(2)$/SBA-15 catalyst. (a) Before reaction. (b) After 6 h on stream.

Table 4
XPS data for various supported Cr_2O_3 catalysts before and after 6 h on stream.

Catalyst	Binding energy (eV)				Percentage (%)			
	Cr(II)	Cr(III)	Cr(V)	Cr(VI)	Cr(II)	Cr(III)	Cr(V)	Cr(VI)
Before reaction								
$Cr_2O_3(2)/ZrO_2$	575.6	576.7	578.5	–	13.6	36.7	49.7	–
$Cr_2O_3(2)$/SBA-15	576.3	576.8	–	579.6	8.3	62.5	–	29.3
$Cr_2O_3(2)/ZrO_2(30)$/SBA-15	575.2	577.3	–	579.6	7.7	74.4	–	17.9
After reaction								
$Cr_2O_3(2)/ZrO_2$ [a]	573.8	575.9	578.8	–	9.4	59.8	30.9	–
$Cr_2O_3(2)$/SBA-15 [a]	574.3	577.5	–	580.5	22.1	42.7	–	35.2
$Cr_2O_3(2)/ZrO_2(30)$/SBA-15 [a]	573.5	577.1	–	580.7	9.9	70.1	–	20.0
$Cr_2O_3(2)$/SBA-15 [b]	–	577.4	579.5	581.7	–	87.4	2.9	9.7
$Cr_2O_3(2)$/SBA-15 [c]	574.5	577.5	–	580.9	13.2	63.2	–	23.6

[a] Non-oxidative dehydrogenation.
[b] Oxidative dehydrogenation by O_2.
[c] Oxidative dehydrogenation by CO_2.

4. Conclusions

The catalytic activity, selectivity and stability of catalysts based on chromia supported on SBA-15 mesoporous silica for non-oxidative and oxidative dehydrogenation of propane are compared with those of Cr_2O_3/ZrO_2, $Cr_2O_3(2)/SiO_2$ and $Cr_2O_3/\gamma\text{-}Al_2O_3$. In non-oxidative dehydrogenation of propane $Cr_2O_3(2)/ZrO_2$ is more active than $Cr_2O_3(2)$/SBA-15 and $Cr_2O_3(2)/ZrO_2(30)$/SBA-15 catalysts, but the latter two are more selective and stable in the reaction. After 6 h on stream the propane conversion and propene yield on $Cr_2O_3(2)/ZrO_2(30)$/SBA-15 at 823 K are 20.9 and 19.4%, respectively. In oxidative dehydrogenation of propane by O_2, $Cr_2O_3(2)$/SBA-15 catalyst is more active and selective than $Cr_2O_3(2)/ZrO_2$ and $Cr_2O_3(2)/\gamma\text{-}Al_2O_3$ catalysts, although the highest propene yield reached at 723 K for the catalyst is only 4.75%. In oxidative dehydrogenation of propane by CO_2, $Cr_2O_3(2)$/SBA-15 catalyst again displays better activity, selectivity and stability in comparison with all the other supported chromia catalysts. After 6 h reaction at 823 K the propane conversion and propene yield on $Cr_2O_3(2)$/SBA-15 is 24.2 and 20.3%, respectively. The strong interaction between chromia and ZrO_2 support stabilizes Cr(V) species on the catalyst surface, produces more monomeric Cr(III) active sites in the reaction and gives rise to an increase in dehydrogenation activity. However, the weak interaction between chromia and the mesoporous silica support and its high specific surface are probably associated with the improvement on selectivity to propene and resistance to coking in the reaction.

Acknowledgments

This work is supported by the Chinese Major State Basic Research Development Program (Grant 7000077500) and the Foundation for University Key Teachers by the Chinese Ministry of Education.

References

[1] F.E. Frey and W.F. Huppke, Ind. Eng. Chem. 25 (1933) 54.
[2] K.K. Kearby, in: *Catalysis*, Vol. 3, ed. P.H. Emmett (Reinhold, New York, 1955) p. 453.
[3] S. De Rossi, G. Ferraris, S. Fremiotti, A. Cimino and V. Indovina, Appl. Catal. A 81 (1992) 113.
[4] S. De Rossi, G. Ferraris, S. Fremiotti, E. Garrone, G. Ghiotti, M.C. Campa and V. Indovina, J. Catal. 148 (1994) 36.
[5] B.M. Weckhuysen and R.A. Schoonheydt, Catal. Today 51 (1999) 223.
[6] M.A. Chaar, D. Patel, M.C. Kung and H.H. Kung, J. Catal. 105 (1987) 483.
[7] C. Mazzochia, C. Aboumrad, C. Diagne, E. Tempesti, J.M. Herrnan and G. Thomas, Catal. Lett. 10 (1991) 181.
[8] J.R.H. Ross, R.H.H. Smits and K. Seshan, Catal. Today 16 (1993) 503.
[9] B. Grzybowska, P. Mkess, R. Grabowski, K. Wcislo, Y. Barbaux and L. Gengembre, Stud. Surf. Sci. Catal. 82 (1994) 151.
[10] F.C. Meunier, A. Yasmeen and J.R.H. Ross, Catal. Today 37 (1997) 33.
[11] M. Baldi, E. Finocchio, C. Pistarino and G. Busca, Appl. Catal. A 173 (1998) 61.
[12] V. Ermini, E. Finocchio, S. Sechi, G. Busca and S. Rossini, Appl. Catal. A 198 (2000) 67.
[13] J. Santamaría-Gonz, J. Mérida-Robles, M. Alcántara-Rodríguez and P. Maireles-Torres, Catal. Lett. 64 (2000) 209.
[14] A. Jiménez-López, E. Rodríguez-Castellón, P. Maireles-Torres, L. Díaz and J. Mérida-Robles, Appl. Catal. A 218 (2001) 295.
[15] I. Takahara and M. Saito, Chem. Lett. (1996) 973.
[16] I. Takahara, W.C. Chang, N. Mimura and M. Saito, Catal. Today 45 (1998) 55.
[17] D. Zhao, J. Feng, Q. Huo, N. Melossh, G.H. Fredrickson, B.F. Chmelka and G.D. Stucky, Science 279 (1998) 548.
[18] D. Zhao, Q. Huo, J. Feng, B.F. Chmelka and G.D. Stucky, J. Am. Chem. Soc. 120 (1998) 6024.
[19] W.M. Hua, Y.H. Yue and Z. Gao, J. Mol. Catal. A 170 (2001) 195.
[20] A. Cimino, D. Cordischi, S. De Rossi, G. Ferraris, D. Gazzoli, V. Indovina, G. Minelli, M. Occhiuzzi and M. Valigi, J. Catal. 127 (1991) 744.